

1 *This is a non-peer reviewed preprint submitted to EarthArXiv*

2 *Article in review at PLOS Water*

3  
4 **Contemporary and Relic Waters Strongly Decoupled in Arid Alpine**  
5 **Environments**

6  
7 Brendan J. Moran (ORCID = 0000-0002-9862-6241)<sup>1</sup>, David F. Boutt (ORCID = 0000-0003-  
8 1397-0279)<sup>1</sup>, Lee Ann Munk (ORCID =0000-0003-2850-545X)<sup>2</sup>, Joshua D. Fisher<sup>3,4</sup> (ORCID =  
9 0000-0003-1054-3132)

10  
11 <sup>1</sup> Department of Earth, Geographic, and Climate Sciences, University of Massachusetts-Amherst,  
12 Amherst, MA, USA

13 <sup>2</sup> Department of Geological Sciences, 3101 Science Circle, University of Alaska-Anchorage,  
14 Anchorage, AK, USA

15 <sup>3</sup> Advanced Consortium on Cooperation, Conflict, and Complexity, Earth Institute, Columbia  
16 University, New York, NY, USA

17 <sup>4</sup> Network for Education and Research on Peace and Sustainability, Hiroshima University,  
18 Higashihiroshima, Japan

19  
20 Corresponding author: Brendan J. Moran ([bmoran@umass.edu](mailto:bmoran@umass.edu))  
21  
22  
23  
24  
25  
26  
27  
28  
29  
30  
31  
32  
33  
34  
35  
36  
37  
38  
39  
40  
41  
42  
43  
44

45 **Abstract**

46           Deciphering the dominant controls on interconnections between groundwater, surface  
47 water, and climate is critical to understanding water cycles in arid environments, yet persistent  
48 uncertainties in the fundamental hydrology of these systems remain. The growing demand for  
49 critical minerals such as lithium and associated water demands in these arid environments has  
50 amplified the urgency to address these uncertainties. We present an integrated hydrological  
51 analysis of the Dry Andes region utilizing a uniquely comprehensive set of tracer data ( $^3\text{H}$ ,  
52  $^{18}\text{O}/^2\text{H}$ ) for this type of environment, paired directly with physical hydrological observations. We  
53 find two strongly decoupled hydrological systems that interact only under specific  
54 hydrogeological conditions where preferential conduits have developed. The primary conditions  
55 in these conduits form are when laterally extensive fine-grained evaporite and/or lacustrine units  
56 or perennial flowing streams exist in connection with groundwater discharge sites. These  
57 conduits which efficiently capture and transport modern or “contemporary” water (weeks to  
58 years old) within the system control the interplay between modern hydroclimate variations and  
59 groundwater aquifers. Modern waters account for a small portion of basin budgets but are critical  
60 to sustaining surface waters due to the existence of these conduits. As a result, surface waters  
61 near basin floors are disproportionately sensitive to short-term climate and anthropogenic  
62 perturbations. This framework describes a new understanding of the dominant controls on  
63 natural water cycles intrinsic to these arid high-elevation systems which improves our ability to  
64 manage critical water resources.

65 **1. Introduction**

66           Water is a scarce but essential resource for human societies and ecosystems in Earth’s driest  
67 regions (Gleeson et al., 2020). Due to the nature of water cycles and hydrogeological systems in

68 these environments, groundwater is an especially critical freshwater resource for both humans  
69 and ecosystems (Bierkens & Wada, 2019; Immerzeel et al., 2020). This is particularly true of  
70 arid, high-elevation regions where steep gradients in topography and climate develop deep water  
71 tables and long transit times leading to the increased importance of multi-decadal groundwater  
72 storage in water budgets (Haitjema and Mitchell-Bruker 2005; Gleeson et al. 2011). In many of  
73 these regions direct (i.e. water extraction) and indirect (i.e. global climate change) anthropogenic  
74 impacts are increasing and threatening the quantity and quality of both groundwater and surface  
75 water (Wang et al., 2018; Zipper et al., 2020). The resulting relative and in some cases absolute  
76 scarcity can increase social tension among riparian parties including communities, governmental  
77 authorities, and industry users (Mehran et al., 2017; Mehran et al., 2015; AghaKouchak et al.,  
78 2015). In addition, responses to natural perturbations (i.e. droughts) are often not well  
79 understood in these environments (Gleeson et al., 2012; Ashraf et al., 2021) making sustainable  
80 and equitable water management challenging. In arid, remote regions, limited precipitation and  
81 the importance of basin-scale groundwater flow systems together with a lack of long-term, high-  
82 quality instrumental records make responsibly allocating water resources challenging (Somers &  
83 McKenzie, 2020; Moran et al., 2022). These conditions also mean that surface water is scarce  
84 and groundwater discharge sourced from relic water (100s to 1000s of years old) often underpins  
85 the hydrological cycle, acting as critical buffers to hydrological systems from large inter-annual  
86 fluctuations (Fan et al., 2013; Bierkens & Wada, 2019; Mcknight et al., 2023). Fundamental  
87 questions remain to be answered about the hydrological functioning of these systems  
88 perpetuating persistent uncertainties around water sources and transport in these environments.  
89 This raises important questions about water scarcity issues in the face of increasing water  
90 resource development and the likely consequences of global climate change.

91           The Dry Andes of South America, marked by one of Earth’s highest and broadest  
92 plateaus on the margin of the driest nonpolar desert, is one of the most extreme places on the  
93 planet (Hartley & Chong, 2002; Rech et al., 2019). This region is often referred to as the  
94 “Lithium Triangle” as it holds a majority of the world’s reserves of the battery component metal  
95 in the form of Li-bearing brines under its salt flats or “Salares” (Munk et al., 2016). The  
96 exploitation of this resource has rapidly expanded in the push to decarbonize the global  
97 economy, highlighting concerns over the sustainability of intensive groundwater extraction  
98 (Gajardo & Redón, 2019; Gutiérrez et al., 2018; Sonter et al., 2020), equitable water  
99 management, and the tradeoffs of water allocation and water management decisions (Crawford et  
100 al., 2021; Diaz Paz, et al. 2023). This landscape is composed of many adjoining endorheic basins  
101 with hyper-arid to arid conditions (<50 mm of precipitation/year) on their basin floors where  
102 groundwater recharge occurs primarily at the highest elevations near watershed divides  
103 (Houston, 2002, 2007, 2009; Boutt et al., 2021). Thick vadose zones (>100 m) across nearly the  
104 entire landscape and intense solar insolation create conditions where actual groundwater  
105 recharge and evaporation rates are difficult to quantify and sources of water difficult to trace  
106 (Rissmann et al. 2015; Scheihing et al. 2018; Viguiet et al. 2020). Where water tables reach the  
107 surface near basin floors, large evaporite deposits, and persistent saline water bodies have  
108 formed (Corenthal et al., 2016; Munk et al., 2021). Persistent surface water features  
109 (saline/brackish lagoons, vegetated wetlands, and perennial and intermittent streams) and their  
110 interconnections are controlled by a combination of lithology, topography, and structure, yet  
111 deciphering the specific controls on connectivity between these features, the modern  
112 hydroclimate and regional groundwater remains elusive (Munk et al., 2021). In addition,  
113 paleoclimate records indicate that at least four major pluvial periods have occurred over the past

114 ~100 ka, increasing precipitation by a factor of 2-3 times modern rates (Gayo et al. 2012;  
115 Placzek et al. 2013). These wet periods dramatically altered the hydrological and ecological  
116 conditions (Pfeiffer et al., 2018), and the effects are likely still evident in the modern  
117 hydrological system in the form of transient groundwater storage changes within the deep and  
118 extensive regional aquifers responding over 100-10,000-year time scales (Moran et. al., 2019).  
119 These conditions have accentuated distinctions between the regional groundwater system and  
120 surface waters, making it an ideal testing ground to address these persistent questions in arid  
121 hydrology.

122         The challenge of hydrological budget closure in these environments has been well  
123 documented worldwide and highlights the uncertainties that remain to be addressed (van Beek et  
124 al. 2011; Liu et al., 2020; Boutt et al., 2021). Imbalances where calculated inflows are smaller  
125 than outflows are observed in nearly every arid region worldwide (Belcher et al., 2009; Ge et al.,  
126 2016; Wood et al., 2015; Kröpelin et al., 2008; Wheatler et al., 2007), including in the massive  
127 Salar de Atacama basin on the western edge of the Andean plateau (Corenthal et al., 2016; Munk  
128 et al., 2018). Major unresolved questions include groundwater transit time characteristics,  
129 surface water sources and residence times, and interconnectivity between groundwater, surface  
130 hydrology, and climate (Favreau et al., 2009; Gleeson et al., 2011; Walvoord et al., 2002).  
131 Recent work in the basins of the Dry Andes has shown that true hydrological catchments often  
132 cross topography and include substantial inputs from relic groundwater sourced from long-flow  
133 paths and/or groundwater storage head-decay (Jordan et al., 2015; Corenthal et al., 2016; Moran  
134 et al., 2019). Therefore, modern water budgets do not come close to closure at steady-state with  
135 modern climate inputs (Boutt et al., 2021). Though the inputs from modern precipitation are  
136 relatively small, large infrequent precipitation events play an important role in sustaining salar

137 floor water bodies in these environments through preferential recharge and areas of restricted  
138 vertical infiltration (Boutt et al., 2016; Munk et al., 2021). Other work shows the critical role that  
139 evaporite stratigraphy has on the expression of surface water features and their connection to  
140 modern precipitation inputs and groundwater discharge (Mcknight et al., 2021; Munk et al.,  
141 2021). Recent work by Moran et al., (2022) establishes that modern water accounts for a  
142 relatively small portion of water budgets but is critical to sustaining surface water bodies and  
143 wetlands, as a result, these arid systems are uniquely sensitive to climate (drought) and  
144 anthropogenic perturbations on short time scales. Much of this work has been focused on the  
145 western edge of the Dry Andes, while other work has explored these issues in basins further east  
146 (Godfrey et al., 2013; Gamboa et al., 2019; Frau et al., 2021) but a mechanistic framework to  
147 explain our observations region-wide has not been established.

148           Substantial gaps remain in our understanding of the time scales and spatial definition of  
149 primary interconnections that constitute water cycles in these environments, specifically the  
150 controls on groundwater, surface water, and modern climate interactions (Masbruch et al., 2016).  
151 We investigate these remaining uncertainties using a large dataset of tritium activity in water  
152 paired with stable oxygen and hydrogen isotope signatures, and hydrophysical and  
153 hydrogeochemical field observations. Utilizing a new approach to integrating and interpreting  
154 the well-established systematics of these tracers we present a process-based conceptual  
155 framework that describes two dominant archetypes of flow systems in these environments and  
156 the controls on connections between their constituent parts. This new framework provides  
157 critical insight into expected responses to perturbations (natural and anthropogenic) in the Dry  
158 Andes and describes intrinsic hydrological processes for arid alpine systems worldwide.

## 159 **2. Methods**

## 160 2.1. Water sample analysis

161 To assess spatially explicit water residence times within these hydrological systems we  
162 utilize stable ( $\delta^{18}\text{O}$  &  $\delta^2\text{H}$ ) and radiogenic ( $^3\text{H}$ ) isotopic tracer measurements in 142 water  
163 samples collected across the Dry Andes. These include surface and groundwaters collected  
164 during numerous field campaigns between October 2011 and March 2021 in Salar de Atacama  
165 (data first presented in Moran et al. 2022) and from 2019 and 2020 on the Puna Plateau. Samples  
166 were collected with a consistent, standardized procedure and in-situ measurements of  
167 temperature, specific conductance, and pH were made at each sampling location during  
168 collection. Tritium activity in water samples was measured at the Dissolved and Noble Gas  
169 Laboratory, University of Utah. Samples were collected in 1 L HDPE bottles with minimal  
170 headspace. In the lab, 0.5 L aliquots were distilled to remove dissolved solids. These water  
171 samples were then degassed in stainless steel flasks until  $<0.01\%$  of dissolved gas remained and  
172 sealed to ingrow helium.  $^3\text{H}$  concentrations were measured by helium ingrowth (Clarke et al.,  
173 1976); 6–12 weeks is typically adequate to ingrow sufficient  $^3\text{He}$  from the decay of  $^3\text{H}$  ( $t^{1/2} =$   
174 12.32 yr.; Lucas & Unterweger, 2000) for analysis.  $^3\text{He}$  concentrations were then measured on a  
175 MAP215-50 magnetic sector mass spectrometer using an electron multiplier to measure low  
176 abundance  $^3\text{He}$ , which was directly correlated with the amount of  $^3\text{H}$  decayed. Data are reported  
177 in tritium units (TU) on the date of sampling, where one TU is equivalent to one tritium atom per  
178  $10^{18}$  hydrogen atoms ( $^3\text{H}/\text{H} \cdot 10^{18}$ ) (Kendall & Caldwell, 1998). Several duplicate analyses of the  
179 same sample were conducted to confirm important values, and the reproducibility for these  
180 samples is of the same order as the precision of the measurement. The analytical error associated  
181 with each sample is reported along with the full dataset in the supplemental material.

182 Water samples were analyzed for  $\delta^2\text{H}$  and  $\delta^{18}\text{O}$  using wave-length scanned cavity ring-  
183 down spectroscopy (Picarro L-1102i); samples were vaporized at 120°C (150°C for higher salt  
184 content waters) in the Stable Isotope Laboratory at the University of Alaska Anchorage.  
185 International reference standards (IAEA, Vienna, Austria) were used to calibrate the instrument  
186 to the VSMOW-VSLAP scale and working standards (USGS45:  $\delta^2\text{H} = -10.3\text{‰}$ ,  $\delta^{18}\text{O} = -2.24\text{‰}$   
187 and USGS46:  $\delta^2\text{H} = -235.8\text{‰}$ ,  $\delta^{18}\text{O} = -29.8\text{‰}$ ) were used with each analytical run to correct for  
188 instrumental drift. Long-term mean and standard deviation records of a purified water laboratory  
189 internal QA/QC standard ( $\delta^2\text{H} = -149.80\text{‰}$ ,  $\delta^{18}\text{O} = -19.68\text{‰}$ ) yield an instrumental precision of  
190 0.93‰ for  $\delta^2\text{H}$  and 0.08‰ for  $\delta^{18}\text{O}$ . The full dataset is provided in the supplemental material.

## 191 **2.2. Tritium Age Tracing Approach**

192 The hydrological system in this region is complex and heterogeneous on all scales, and  
193 large gaps exist in hydrogeological and hydroclimatological data coverage, especially above the  
194 basin floors at the higher elevation plateaus and mountain peaks. Very deep water tables (100s of  
195 meters) and rugged terrain make direct observation of the groundwater system impractical across  
196 much of the landscape. Long-term high-quality terrestrial monitoring of climatology and  
197 streamflow flow is also sparse. Therefore, highly parameterized models and tracers that require  
198 additional assumptions are not the most effective tools to assess water flux rates or transit times  
199 in this environment. Tracing signatures recorded in the water molecule itself most reliably  
200 integrate small-scale variability with large-scale processes and can be captured with individual  
201 water samples (Birkel et al., 2015; Buttle, 1994). Stable isotope ratios ( $\delta^{18}\text{O}$ ,  $\delta^2\text{H}$ ) and  
202 radioisotopes ( $^3\text{H}$ ) in water offer many unique advantages in these systems (Cook & Bohlke,  
203 2000; Kendall & Caldwell, 1998). Besides the well-understood influence (fractionation) from  
204 low and high-temperature water-rock interaction and evaporation, signatures of  $\delta^{18}\text{O}$  &  $\delta^2\text{H}$  in



205 groundwater recharge remain unchanged from infiltration until re-emergence from the ground  
206 (Beria et al., 2018; Clark & Fritz, 1997; Kendall & McDonnell, 1998). Geothermal water-rock  
207 interactions cause a pronounced “oxygen shift” in  $\delta^{18}\text{O}$  &  $\delta^2\text{H}$  cross-plot space and a trend line  
208 with a slope approaching zero (Panichi and Gonfiantini, 1977). Evaporation causes the signature  
209 of a water parcel to increase in deuterium-excess and deviate from the GMWL along a steep,  
210 positive linear slope. Deuterium excess (d-excess) is the deviation from the global meteoric water  
211 line defined as  $\text{d-excess} = \delta^2\text{H} - 8 * \delta^{18}\text{O}$  (Dansgaard, 1964). These fractionation processes both  
212 act to progressively increase the d-excess value in a sample or group of samples but can be  
213 reliably differentiated from each other through comparison of the slopes of the apparent local  
214 evaporation line trends (LEL) defining groups of samples (Rissmann et al., 2015, Moran et al.,  
215 2019).

216 Radioisotope signatures ( $^3\text{H}$ ) are also conservative but follow a predictable decay (half-  
217 life of 12.32 years) during transit. To effectively utilize this tracer, we must constrain the  $^3\text{H}$   
218 content of modern precipitation, this defines the signature of direct modern inputs to the  
219 hydrologic system. Widespread atmospheric nuclear bomb testing in the late 1950s and early  
220 '60s created a large and unmistakable peak in global atmospheric  $^3\text{H}$  concentrations which  
221 increased activities in precipitation globally by greater than an order of magnitude (Cartwright et  
222 al., 2017). We assume the modern value in precipitation described above is representative of  
223 average precipitation from about 2000 to the present since the bomb peak signature is no longer  
224 resolvable after that date in the Southern Hemisphere (Rooyen et al., 2021). This modern  
225 signature is also representative of precipitation before the mid-1950s since the bomb peak had  
226 not yet occurred (Houston, 2007; Jasechko, 2016). This period of high  $^3\text{H}$  activity in  
227 precipitation and therefore in recharge during that time allows for reliable differentiation

228 between water recharged post-1955 and that before 1955 because if this strong signature is not  
229 observed in water (very low  $^3\text{H}$  activity), very little if any of that water is composed of recharge  
230 after the bomb peak. Since the  $^3\text{H}$  activity in any given sample is a bulk sample representing  
231 mixtures of unknown sources and respective amounts, we must also be careful not to over-  
232 interpret specific  $^3\text{H}$  activities in individual samples without proper physical constraints.  
233 Therefore, to ensure a reliable and conservative interpretation of this broad dataset we determine  
234 a simple “percent modern water” ratio in each sample as the ratio of modern precipitation input  
235 activity to the activity measured in the sample. Using the  $^3\text{H}$  activity in modern precipitation, we  
236 determine the proportion of modern or “contemporary” and pre-modern or “relic” water  
237 components in the sample according to the formula: *Percent Modern Water in Sample* =  
238 
$$\frac{{}^3\text{H Activity in Sample}}{{}^3\text{H Activity in Modern Precipitation}}$$

239 The  $^3\text{H}$  activities in modern precipitation over the region, also presented by Boutt et al.  
240 (2016) and Moran et al. (2019), are determined to be  $3.17 \pm 0.53$  TU from 5 amount-weighted  
241 rain and snow samples collected between 2013 and 2014 in the western part of the region  
242 (Chile); and determined to be  $4.54 \pm 1.34$  TU from 3 amount-weighted rain and snow samples  
243 collected between 2018 and 2019 in the eastern region (Argentine Puna) (**Figure 1**). These  
244 values are within the range reported by others in the region (Cortecci et al., 2005; Grosjean et al.,  
245 1995; Herrera et al., 2016; Houston, 2002, 2007). Consistent with other studies in this region and  
246 across the southern hemisphere, the  $^3\text{H}$  activities in precipitation have now stabilized to reflect  
247 modern production and so this value accurately reflects (within uncertainty) any recharge that  
248 occurred within the last few decades (Basaldúa et al., 2022). Water recharged in 1955 before the  
249 bomb peak with a  $^3\text{H}$  activity of  $3.17 \pm 0.53$  TU would have between 0.07 and 0.10 TU in June  
250 2020, or about 2-3% of the modern precipitation input; water with a  $^3\text{H}$  activity of  $4.54 \pm 1.34$

251 TU would have between 0.08 and 0.15 TU in June 2020, also about 2-3% of the modern  
 252 precipitation input (Stewart et al., 2017). Due to the small but non-negligible analytical  
 253 uncertainty ( $\sim 0.02\text{-}0.07$  TU at low activities), samples with these very small activities are herein  
 254 considered to be effectively  $^3\text{H}$ -dead waters or indistinguishable from zero. Waters registering  
 255 such low activities are assumed to contain negligible volumes of water recharged post-bomb

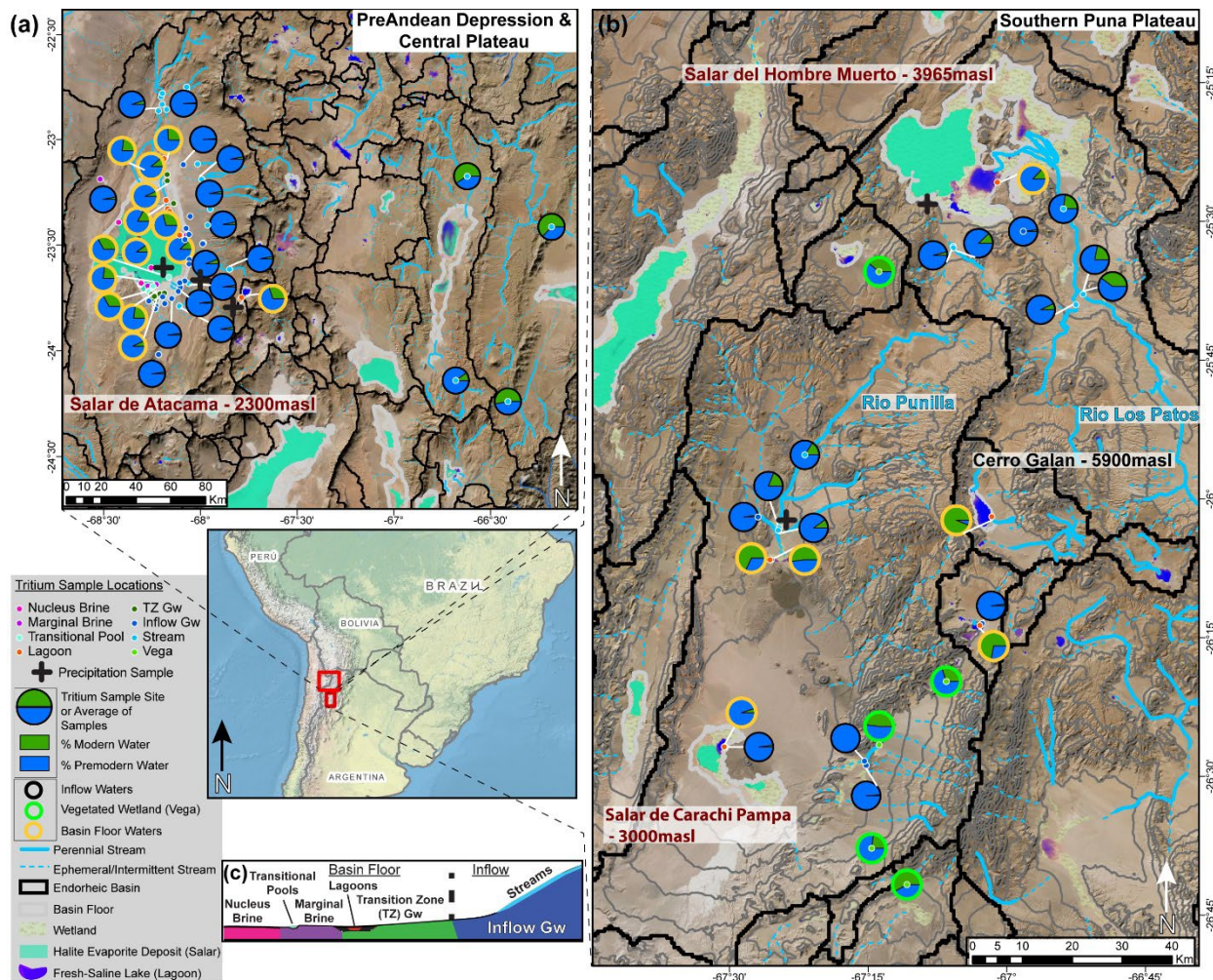


**Figure 1.** Surface and groundwaters in the Dry Andes analyzed for  $^3\text{H}$ ,  $\delta^{18}\text{O}$ , and  $\delta^2\text{H}$  in this study ( $n=142$ ). Pie charts represent percent modern content, colored outlines show general water type groupings and colored dots show sample sites and their physical water type. The black crosses are precipitation sample sites used in  $^3\text{H}$  analysis. Black outlines show internally drained basins, blue solid lines are perennial streams, and blue dashed lines are intermittent streams. Important features (salar, mountains, rivers) are noted along with their elevations. (a) Map of the Salar de Atacama basin and the northern Puna region to the east, where pie charts represent average content of inflow zones and surface waters in order to display all data (see Moran et al., 2022). (b) Map of the southern Puna where each pie chart represents one sample. (c) A schematic cross-section of salar-basin floor hydrogeological systems describing the physical water classifications.

256 peak (1955), as even small amounts of water with these higher activities would heavily skew  
257 resultant activities in these  $^3\text{H}$ -dead samples to appear to contain high levels of modern water.  
258 Since most of the waters measured in this environment contain effectively no  $^3\text{H}$ , our objective is  
259 not to directly estimate discrete mean residence time distributions but instead to describe the  
260 relative proportions of  $^3\text{H}$ -dead to recent recharge (<65 years old) in these waters (Cartwright et  
261 al., 2017). This relative water age value allows for the reliable interpretation of connections to  
262 modern precipitation inputs, as well as the lack thereof.

### 263 **3. Results & Discussion**

#### 264 **3.1. Physical water-type groupings**

265 Sampled waters were grouped into seven physical water types. These distinctions are  
266 based on extensive knowledge of the regional hydrogeology gathered during more than ten field  
267 campaigns in Salar de Atacama on the Puna Plateau, previously published works, and scrutiny of  
268 geochemical signatures (Munk et al., 2021). A schematic cross-section describing these water  
269 groupings is shown in **Figure 1c**. Nucleus Brines are groundwaters from the core of the halite-  
270 dominated brine aquifer, sampled at shallow depths <13 meters below ground level (mbgl),  
271 Marginal Brines are groundwaters from the margins of the brine aquifer, sampled at the water  
272 table (<2 mbgl). Transitional Pools are highly saline, shallow pools that form at the margin of the  
273 halite crust that grow and shrink rapidly primarily in response to precipitation events. These are  
274 often adjacent to (~1-2km away) but distinct from the Lagoons (saline lakes). Many of these  
275 Lagoon water bodies also grow and shrink seasonally and after precipitation events but are  
276 perennially extant. They are also quite shallow (<1m) but much less saline than the Transitional  
277 Pools. In Salar de Atacama we were able to access groundwater wells, whereas, in the Puna  
278 region, these brine bodies are present in the vicinity of the salars indicated in **Figure 1**, there are

279 currently very few accessible groundwater wells that could be sampled. In addition, on the high-  
280 elevation plateau, there are no true Transitional Pools as there are in Salar de Atacama. The  
281 waters classified as “inflows” are separated into three groups; Streams are perennially and  
282 intermittently flowing fresh surface waters, Inflow Groundwaters (Inflow Gw) are fresh to  
283 brackish waters sampled from wells and from persistent springs that we define as groundwater  
284 outcrops, and Transition Zone Groundwaters are brackish to saline waters sampled at the water  
285 table within the transition zone between the inflow water bodies and the brines.

### 286 **3.2. Water transit time partitioning**

287 We assess tritium ( $^3\text{H}$ ) activities in 142 samples representing all major physical water  
288 types covering a large swath of the Dry Andes. In this environment where modern water and pre-  
289 modern water appear to be strongly decoupled in terms of where they exist on the landscape,  
290 determining the relative proportion of each in a sample is a highly effective way to define the  
291 relative transit age and therefore sources of water to different water bodies. A detailed summary  
292 of this analysis and the raw and derived data presented in the results is provided in the  
293 supplemental material (**Table S1**).

294 The geographical distribution of relative water age across the region highlights important  
295 results concerning surface and groundwater on basin floors and inflow waters to the basins  
296 (**Figure 1**). First, in the Salar de Atacama basin, all basin inflow waters (streams, springs, and  
297 groundwaters) are principally composed of pre-modern water (ie. 0-5% modern; Moran et al.,  
298 2022). Relative modern water components in inflow waters are consistent across several years,  
299 and in different seasons of site repeat sampling, larger river waters show higher seasonal and  
300 yearly variability due to their direct and more rapid interaction with modern precipitation inputs  
301 (**Figure S1**). Waters at the basin floor, in saline surface waters, and brine groundwaters also

302 show consistently larger components of modern water. In addition, two high-elevation (4100  
303 masl) fresh-to-brackish lakes near the watershed divide contain ~30% modern water, similar to  
304 the basin floor surface waters. These results demonstrate the strong distinctions that exist  
305 between overall inputs to these basin water budgets and the near-surface waters at the basin  
306 floors, especially since recent inflow waters are critical to sustaining these surface waters. These  
307 general observations also describe the higher-elevation plateau endorheic basins to the east.  
308 Inflow groundwaters, which here consist of spring complexes that are effectively “outcrops” of  
309 and discharge from the groundwater system to the surface, have very low modern water content  
310 (0-2%). Basin floor waters on the plateau (saline surface waters) also have substantially higher  
311 modern water content than the nearby groundwaters.

312         There are a few important distinctions between water age distributions on the plateau and  
313 at the lower elevation of Salar de Atacama. One is that many of these higher elevation basin floor  
314 waters (brackish-brine lagoons) have modern water contents of >50%, some of the highest values  
315 observed in the region. Two exceptions to this are the lagoons at Salar del Hombre Muerto and  
316 Salar del Carachi Pampa. Another key distinction is the consistently high modern water content  
317 in streams on the Puna plateau, particularly in the large perennial rivers of Rio Los Patos and Rio  
318 Punilla which average ~22% modern, and streams in the northern Puna region which average  
319 46%. The vegetated wetland complexes above the basin floors, common to the high elevations of  
320 this region, have consistently higher modern water content than nearby groundwaters and  
321 streams. The commonalities in transit age across the whole region and the distinctions between  
322 low-elevation and high-elevation systems are valuable in deciphering the dominant controls on  
323 water transport and interconnectivity.

324 Examining the distribution of these data across the region allows for further examination  
 325 of common dominant controlling mechanisms across the many individual basin systems.  
 326 Kruskal-Wallis tests were conducted on data groupings in each panel of **Figure 2** showing that  
 327 the groupings chosen are statistically unique (P-value <0.001) except when grouped by Sample  
 328 Elevation Above Basin Floor (P-value=0.09), detailed results of these tests are provided in the  
 329 supplemental material (**Table S2**). **Figure 2a** shows the distribution of the water age ratios  
 330 grouped by water type, a definition based on the position between recharge and discharge zone,  
 331 and salinity (described schematically in **Figure 1c**). Inflow groundwaters average <5% modern  
 332 water content, similar to stream waters yet stream data skew towards very low modern water

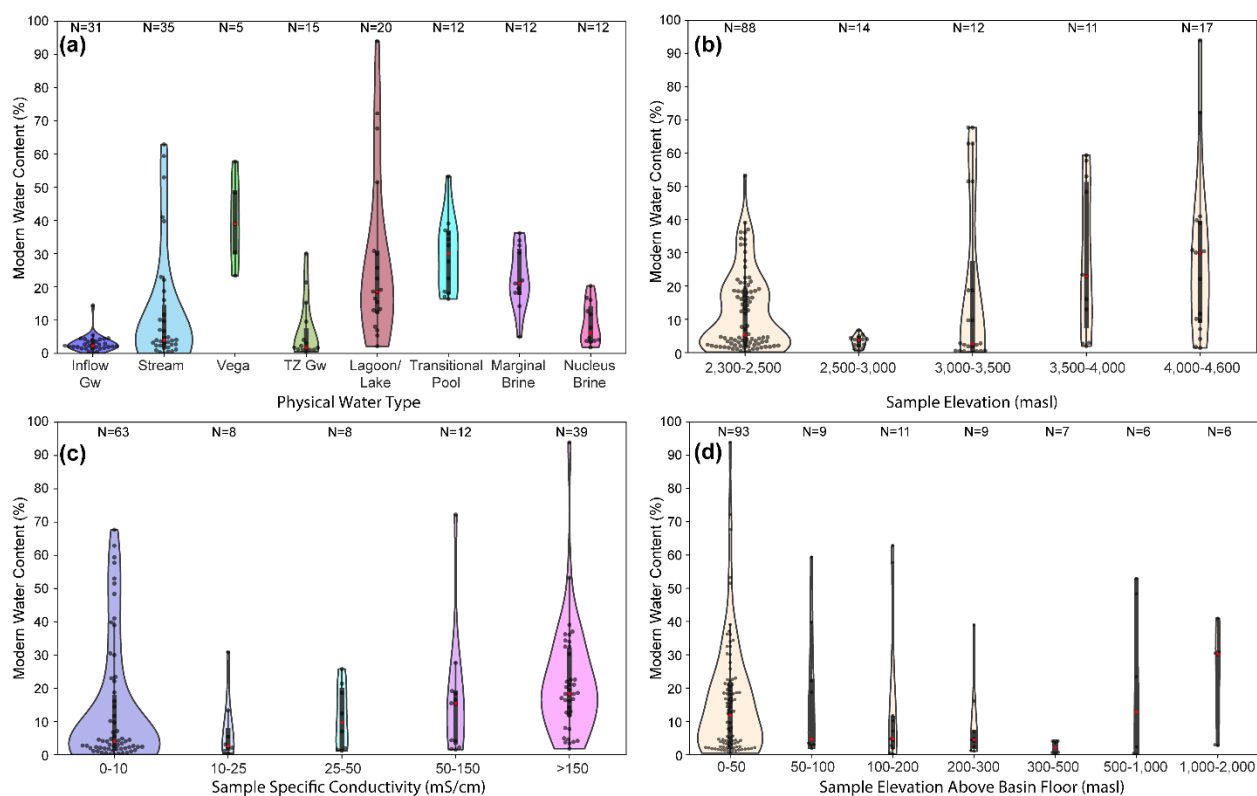


**Figure 2.** Statistical distributions of  $^3\text{H}$ -derived percent modern water results. Grey boxes inside the polygons show the interquartile range; red dots are the median and polygons represent the frequency distribution of the data (black dots). Data grouped by (a) physical water type, where colors of polygons correspond to physical water type dots in Figure 1; (b) by elevation of sample; (c) by specific conductance of sample, where colors of polygons show fresh (blue) to brine (pink) waters; and (d) by sample elevation above the basin floor (basin floor elevations indicated in Figure 1).

333 values. Importantly several stream samples show higher modern water content of between 15%  
334 and 60%, these samples are of the large perennial streams mentioned above. Saline surface  
335 waters near the basin floors average 20-30% modern while the lagoons (perennial saline lakes) in  
336 particular show a large range in values but also skew towards the lower values. The brine  
337 groundwater bodies within the salar evaporites and the brackish groundwaters in the transition  
338 zone between fresh inflow and brine (TZ Gw) show two primary groupings of relative age. One  
339 of very low modern water content and the other close to 25% modern, this younger water  
340 component is most clearly shown in the marginal brine waters but is also present in the other two  
341 water bodies. Grouped by sample elevation we observe that on average, more modern water  
342 exists near the surface above 3000 masl but also that waters with very small modern components  
343 are present at all elevations (**Figure 2b**). Importantly the lowest elevations show clusters of  
344 samples with modern content similar to the highest elevations. These characteristics can also be  
345 seen when grouped by elevation above the basin floor (**Figure 2d**), where samples collected  
346 highest above the basin floor average higher modern water content. Most samples were collected  
347 very near basin floors, which reflects the concentration of near-surface water and its absence  
348 elsewhere, and shows a wide distribution of water ages. Grouped by specific conductivity (a  
349 proxy for salinity) we see that the freshest water is predominately relic but also that there are  
350 many freshwaters with much higher modern content. Average water age generally increases with  
351 salinity but the saltiest waters (brines) also contain a range of ages from <3% modern to nearly  
352 95% modern. These results provide many important insights into where pre-modern and modern  
353 water persist in this system, their sources, and how they interact.

354           These results highlight the strong influence of hydroclimate, topography, and  
355 hydrogeology on transit time and interaction with modern inputs. In this arid environment,



356 modern water is not spatially common but differences in climate across the region have  
357 important influences on surface hydrology. Region-wide, groundwaters, and most streams have  
358 very small modern components reflecting the long transit times from their source waters. But the  
359 large perennially flowing streams that exist at the colder and slightly wetter climate at these  
360 higher elevations, have a substantial portion of their flow composed of modern water. Vegetated  
361 wetland complexes or vegas can be extensive and often form near basin floors at the periphery of  
362 salars, high elevation wetlands or peatlands referred to in this region as bofedales also occur  
363 sporadically on the Puna above 3800 masl around groundwater outcrops or springs (Marconi et  
364 al., 2022). Although these two systems are characterized by different ecology, they display  
365 similar hydrological characteristics in that they are strongly influenced by recent precipitation  
366 inputs; we refer to all these systems together herein as vegas. The consistently strong signature in  
367 surface water bodies at basin floors exists across the region but the climate at higher elevations  
368 appears to create conditions where less than half of their water is composed of regional  
369 groundwater. Specific hydrogeological and ecological conditions that allow water tables to  
370 persist close to the surface (<5m) are a shared feature of all of the water bodies mentioned above.  
371 We argue that these conditions strongly control how modern water enters and moves through this  
372 system since most precipitation either evaporates in the thick vadose zones or slowly infiltrates  
373 towards the groundwater table below.

### 374 **3.3. Hydrogeological mechanisms controlling source partitioning**

375 We further investigate mechanisms controlling the partitioning of waters in this  
376 environment using d-excess signatures paired with percent modern water content (**Figure 3a**).  
377 The d-excess provides a reliable measure of the amount of evaporation a sampled water has  
378 undergone, placing important constraints on waters that have had little or no atmospheric

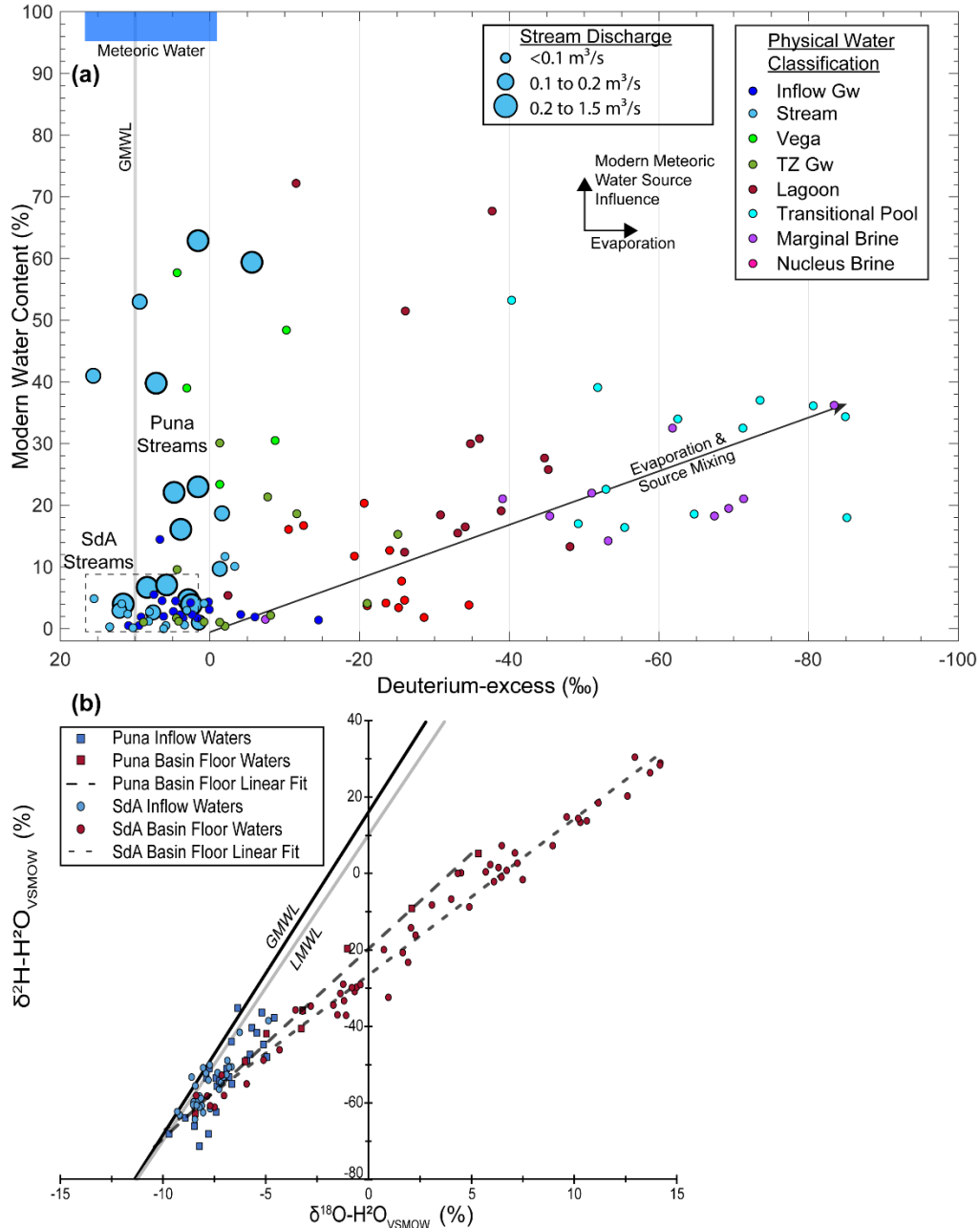


**Figure 3.** (a) Processes controlling physical water distinctions and interactions based on  $^3\text{H}$ ,  $\delta^{18}\text{O}$ , and  $\delta^2\text{H}$  signatures. Circles are proportional to the average magnitude of discharge at each stream site, SdA streams plot within the black dashed box. The grey vertical bar is the Global Meteoric Water Line (GMWL), and the blue box at the top represents the approximate range of meteoric input waters in the region (based on Moran et al., 2019 data). Arrows depict the influence of important hydrological processes and interactions. (b) Shows these data plotted in  $\delta^{18}\text{O}-\delta^2\text{H}$  space relative to the LMWL (Rissmann et al. 2015) and evaporation trends of basin floor waters in Salar de Atacama and on the higher elevation Puna plateau.

379 interaction from that which has undergone substantial evaporation (waters with increasing

380 negative values). We group all stream samples by average streamflow at the sample site to

381 highlight the relative size of each stream and therefore the relative volume of modern water  
382 represented by the ratio (data provided in **Tables S3**).

383           The inflow groundwaters plot close to the Global Meteoric Water Line (GMWL) as they  
384 are composed of infiltration that interacted minimally with the atmosphere before becoming  
385 groundwater, and their modern water content indicates nearly all of their volume is composed of  
386 relic water. The streams also plot along the GMWL and most have similar mean age profiles to  
387 the inflow groundwaters while some have many times the amount of modern water in them. This  
388 likely reflects the fact that inflow groundwater is relic regional groundwater and provides the  
389 baseflow to streams in this environment. But some of the streams, particularly the large streams  
390 on the Puna plateau are composed of a large amount of recent meteoric water that does not show  
391 a strong evaporation signature. The vegas also have a similar signature to these large Puna  
392 streams. The other major water groupings display a few distinctive characteristics. Marginal  
393 brines and transitional pools plot in a similar position likely reflecting similar sources and  
394 interactions between these water bodies. The nucleus brine waters show less evaporation,  
395 indicating a distinct combination of sources but skew more towards the regional groundwaters  
396 than the marginal water bodies. The lagoon waters tend to fall between the nucleus brines and  
397 the marginal/transitional pool waters with a large range of modern components and are less  
398 evaporated than the other saline surface waters suggesting they are more closely connected to the  
399 inflow waters than other basin floor water bodies.

400           These results reiterate that most inflow is relic water but also show that large streams  
401 particularly on the higher elevation plateau can transport substantial volumes of modern water  
402 relatively quickly through these systems. These streams along with the vegetated wetland

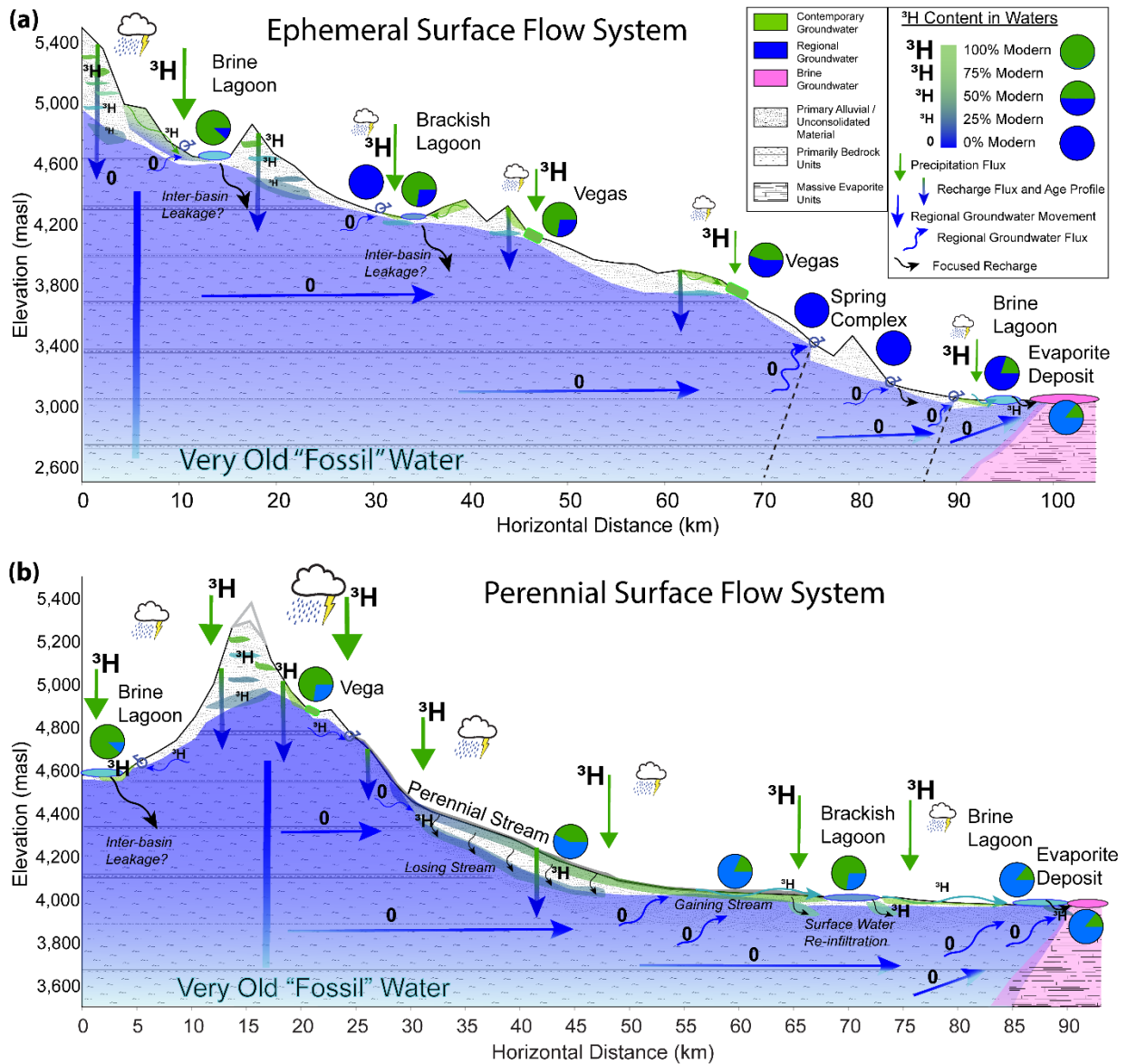


**Figure 4.** Conceptual model of archetypal flow regimes in the Dry Andes. Size of the  $^3\text{H}$  symbol and pie charts show relative modern water content in major water bodies and along flow paths. Arrows show general flow paths from precipitation-to-recharge-to-groundwater colored by relative modern water content from green-to-blue with predicted presence of very old “Fossil” water in teal. Straight arrows show general modern precipitation inputs and regional groundwaters, and zig-zag arrows represent water fluxes to and from the surface scaled by relative flux magnitude. General water body types and geology are colored and textured. (a) Represents the archetype dominated by ephemeral streams and regional groundwater fluxes, (b) represents the archetype dominated by perennial streams that act as efficient conduits for modern water.

403 complexes appear to be the primary hydrological conditions under which fresh modern water is

404 captured and transported within human time scales. The fact that the saline basin floor surface

405 water bodies also contain substantial amounts of modern water and that these four water types

406 (streams, vegas, lagoons, and transitional pools) are the only places where water tables exist near  
407 the surface in this environment demonstrates this is the primary pathway of modern hydroclimate  
408 connection to the larger hydrological cycle. We present the two principle archetypal frameworks  
409 that describe these climate-surface water-groundwater interactions in this system.

410 We define the archetypal flow systems in this environment which describe and integrate  
411 our observations of transit time and flow paths in the Dry Andes (**Figure 4**). The Ephemeral  
412 Surface Flow System is the more common type and is defined by steep topography and structural  
413 and hydrogeological conditions that promote infiltration and drop water tables well below the  
414 surface (**Figure 4a**). Intermittent streams do often form downgradient of spring complexes in  
415 these systems (for example in the southern and eastern parts of the Salar de Atacama and to the  
416 east of Salar de Carchi Pampa) but generally flow for short distances downgradient of spring  
417 discharge and/or intermittently during large rain events. These streams are fed almost entirely by  
418 regional groundwater and contain very small or transitory proportions of modern water. Perched  
419 aquifers do form, in the vicinity of vegetated wetlands at elevation and particularly near the basin  
420 floors where the abundance of fine-grained deposits and evaporite precipitation prevents  
421 infiltration directly to the deeper water table, these perched aquifers allow moderately aged  
422 (years-decades) waters to feed basin floors and importantly create persistent shallow water tables  
423 that allow recent rainfall to mix with the saturated zone near the surface. We argue that these  
424 conditions are what maintain the vegetated wetlands and lagoons at elevation and allow them to  
425 capture and transmit modern precipitation. The dimensions and depth of the water table  
426 constitute the dominant control on surface water formation and modern hydroclimate  
427 connections in these systems.

428           The other primary archetype in this environment is a perennial surface flow system which  
429 is defined primarily by relatively large perennial streams that are also fed predominantly by  
430 regional groundwater (baseflow) but maintain consistent flow in all seasons and over large  
431 distances (30-100 km) (**Figure 4b**). Smaller topographic gradients and/or hydrological  
432 conditions that allow these streams to form create unique hydrological systems that capture more  
433 modern rainfall and move it efficiently toward basin floors. The presence of this perennial  
434 surface water itself, like shallow water tables, creates conduits that capture modern rainfall and  
435 runoff before it evaporates or begins infiltrating through the thick vadose zones. The presence of  
436 these conduits is the primary control on connections between the modern hydroclimate and  
437 surface waters in these systems. Across most of this arid landscape, when rainfall does occur,  
438 much of it rapidly evaporates at the surface and as it makes its way toward the water table, the  
439 0.01-5% of that water that reaches the water table as groundwater recharge (now and during past  
440 climate conditions) sustains the regional groundwater system (Scanlon et al., 2006; Boutt et al.,  
441 2021). These mechanisms are also responsible for maintaining the saline water bodies near the  
442 basin floors and on the salars. Groundwater discharge is focused near the basin floor where the  
443 topography flattens and fine-grained units have accumulated, creating permeability contrasts that  
444 both force water to the surface and restrict infiltration. These conditions create persistent shallow  
445 water tables that in turn allow modern waters to efficiently mix with relic groundwaters.

#### 446           **3.4. Implications for society and ecosystems**

447           The extreme decoupling between basin-to-regional scale groundwaters, which constitute  
448 the primary inflow to these endorheic basins, and local, modern precipitation inputs has major  
449 implications for the management and future sustainability of water systems in the Dry Andes and  
450 other arid mountain environments. Our results show that modern precipitation comprises only a

451 small portion of modern hydrological budgets in these environments but is critical to maintaining  
452 surface water bodies and vegetation due to a unique but intrinsic set of hydrogeological  
453 conditions. The Sixth Assessment Report from the Intergovernmental Panel on Climate Change  
454 (IPCC) reports a high confidence projection of increased drought extent and severity in the area  
455 (IPCC 2022), which presents threats to the delicate balance of these environments and  
456 hydrological systems. Prolonged droughts have been shown to cause major and rapid changes to  
457 surface water systems in this region over the last few decades (Frau et al., 2021; Moran et al.,  
458 2022). It is critical to understand the current interplay between pre-modern and modern waters to  
459 define how human use and changing temperature and precipitation in the region could alter the  
460 integrity of these systems. We define the modern and relic water systems in this region for the  
461 first time within a framework that reconciles the prevalence of relic groundwater in these  
462 environments with the observations of rapid changes to surface waters in response to natural and  
463 anthropogenic perturbations.

464         A major focus in these watersheds is the interplay between competing use of water by a  
465 variety of riparian stakeholders and the policies and use rights conferred by water managers.  
466 Demands for water resources exist from current metal mines and the massive expansion of  
467 exploration for lithium among other commodities, indigenous communities, agriculture, as well  
468 as the environmental flows required to maintain existing ecosystem services and functions. There  
469 is a lack of watershed-specific knowledge of water resources in the region, meaning that water  
470 management is naïve to the pre-modern and modern water balance dynamics. If left unfilled, this  
471 knowledge gap could lead to use patterns that threaten the viability of these hydrological  
472 systems. Moreover, there is limited regional coordination and oversight related to water  
473 management in the area which exacerbates the sustainable water management challenge.

474           The work presented in this study provides an important starting point for filling the  
475 technical knowledge gap surrounding water balances in these environments. The present work  
476 develops a general framework for users of water in these basins and presents the opportunity to  
477 revise water budgets within scientifically justifiable frameworks that do not require steady-state  
478 closure of basin budgets to allocate water resources more responsibly. In addition, this new  
479 understanding can greatly improve our ability to attribute current and future impacts from  
480 anthropogenic activities in fragile wetlands systems and predict and respond more effectively to  
481 the accelerating impacts of human-induced climate change. This analysis and the new  
482 hydrological conceptual models we present will improve our ability to reduce the risk of  
483 depleting vulnerable freshwater resources and damaging ecosystems reliant on the delicate  
484 balance between modern and pre-modern water inputs and plan human development that avoids  
485 the most damaging potential impacts on water quantity and quality. For instance, a particular  
486 focus with high potential benefit would be to prioritize the protection of these modern water  
487 conduits from disruption or obstruction and/or the removal of existing obstructions. An  
488 understanding of connections to modern and past climates will also improve our ability to plan  
489 for the effects of future climate changes in these environments.

#### 490 **Data Availability**

491 All data necessary to interpret, replicate, and build upon the findings reported in this article are  
492 provided as tables in the supplemental information.

#### 493 **References**

494 AghaKouchak, A., Feldman, D., Hoerling, M., Huxman, T. & Lund, J. Water and climate:  
495 Recognize anthropogenic drought. *Nature* 524, 409–11 (2015).



- 496 Ashraf, S., Nazemi, A., & AghaKouchak, A. (2021). Anthropogenic drought dominates  
497 groundwater depletion in Iran. *Scientific Reports*, 11(1), 9135.  
498 <https://doi.org/10.1038/s41598-021-88522-y>
- 499 Basaldúa, A., Alcaraz, E., Quiroz-Londoño, M., Dapeña, C., Ibarra, E., Vélez-Agudelo, C., ...  
500 Martínez, D. (2022). Reconstruction of the record of tritium in precipitation in the  
501 temperate zone of South America. *Hydrological Processes*, 36(9), 1–11.  
502 <https://doi.org/10.1002/hyp.14691>
- 503 van Beek, L. P. H., Wada, Y., & Bierkens, M. F. P. (2011). Global monthly water stress: 1.  
504 Water balance and water availability. *Water Resources Research*, 47(7), n/a-n/a.  
505 <https://doi.org/10.1029/2010WR009791>
- 506 Belcher, W. R., Bedinger, M. S., Back, J. T., & Sweetkind, D. S. (2009). Interbasin flow in the  
507 Great Basin with special reference to the southern Funeral Mountains and the source of  
508 Furnace Creek springs, Death Valley, California, U.S. *Journal of Hydrology*, 369(1–2),  
509 30–43. <https://doi.org/10.1016/j.jhydrol.2009.02.048>
- 510 Beria, H., Larsen, J. R., Ceperley, N. C., Michelon, A., Vennemann, T., & Schaeffli, B. (2018).  
511 Understanding snow hydrological processes through the lens of stable water isotopes.  
512 *Wiley Interdisciplinary Reviews: Water*, (June), e1311.  
513 <https://doi.org/10.1002/wat2.1311>
- 514 Bierkens, M. F. P., & Wada, Y. (2019). Non-renewable groundwater use and groundwater  
515 depletion: a review. *Environmental Research Letters*, 14(6), 063002.  
516 <https://doi.org/10.1088/1748-9326/ab1a5f>
- 517 Birkel, C., & Soulsby, C. (2015). Advancing tracer-aided rainfall-runoff modelling: a review of  
518 progress, problems and unrealised potential. *Hydrological Processes*, 29(25), 5227–5240.  
519 <https://doi.org/10.1002/hyp.10594>
- 520 Boutt, D. F., Hynek, S. A., Munk, L. A., & Corenthal, L. G. (2016). Rapid recharge of fresh  
521 water to the halite-hosted brine aquifer of Salar de Atacama, Chile. *Hydrological  
522 Processes*, 30(25), 4720–4740. <https://doi.org/10.1002/hyp.10994>
- 523 Boutt, D.F., Corenthal, L.G., Moran, B.J. et al. Imbalance in the modern hydrologic budget of  
524 topographic catchments along the western slope of the Andes (21–25°S): implications for  
525 groundwater recharge assessment. *Hydrogeol J* 29, 985–1007 (2021).  
526 <https://doi.org/10.1007/s10040-021-02309-z>
- 527 Buttle, J.M. (1994). Isotope hydrograph separations and rapid delivery of pre-event water from  
528 basins drainage. *Phys. Geogr.* 18, 16–41.
- 529 Cartwright, I., Cendón, D., Currell, M., & Meredith, K. (2017). A review of radioactive isotopes  
530 and other residence time tracers in understanding groundwater recharge: Possibilities,  
531 challenges, and limitations. *Journal of Hydrology*, 555, 797–811.  
532 <https://doi.org/10.1016/j.jhydrol.2017.10.053>
- 533 Clark, I. & Fritz, P. (1997). *Environmental Isotopes in Hydrogeology*. Lewis Publications, Boca  
534 Raton, FL.

- 535 Clarke, W.B., Jenkins, W.J., Top, Z. (1976). Determination of tritium by mass spectrometric  
536 measurement of  $^3\text{He}$ . *Int. J. Appl. Radiat. Isot.* 27 (9), 515e522.
- 537 Cook, P.G. and Bohlke, J.K. (2000). Determining timescales for groundwater flow and solute  
538 transport. In: Cook, P.G., Herczeg, A.L. (Eds.), *Environmental Tracers in Subsurface*  
539 *Hydrology*. Kluwer, Boston, pp. 1–30.
- 540 Corenthal, L. G., D. F. Boutt, S. A. Hynek, and L. A. Munk (2016), Regional groundwater flow  
541 and accumulation of a massive evaporite deposit at the margin of the Chilean Altiplano,  
542 *Geophys. Res. Lett.*, 43, doi:10.1002/2016GL070076
- 543 Cortecci, G., Boschetti, T., Mussi, M., Lameli, C. H., Mucchino, C., & Barbieri, M. (2005). New  
544 chemical and original isotopic data on waters from El Tatio geothermal field, northern  
545 Chile. *Geochemical Journal*, 39(6), 547–571. <https://doi.org/10.2343/geochemj.39.547>
- 546 Crawford, Alec Lunde Seefeldt, Jennapher, Kent, Richard, Helbert, Maryse, Pimentel, Guzmán,  
547 Gonzalo, González, Alejandro, Chen, Zheng, and Andy Abbott. (2021) Lithium: The big  
548 picture. *One Earth* 4(3): 323-326. <https://doi.org/10.1016/j.oneear.2021.02.021>
- 549 Dansgaard, W. (1964), Stable isotopes in precipitation, *Tellus*, 16(4), 436–468,  
550 doi:10.1111/j.2153-3490.1964.tb00181.x.
- 551 Díaz Paz, Walter Fernando., Escosteguy, Melisa., Seghezze, Lucas., Hufty, Marc., Kruse,  
552 Eduardo., and Martín Alejandro Iribarnegaray, (2023). Lithium mining, water resources,  
553 and socio-economic issues in northern Argentina: We are not all in the same boat.  
554 *Resources Policy* 81 (2023): 103288, <https://doi.org/10.1016/j.resourpol.2022.103288>
- 555 Favreau, G., Cappelaere, B., Massuel, S., Leblanc, M., Boucher, M., Boulain, N., & Leduc, C.  
556 (2009). Land clearing, climate variability, and water resources increase in semiarid  
557 southwest Niger: A review. *Water Resources Research*, 45(7), 1–18.  
558 <https://doi.org/10.1029/2007WR006785>
- 559 Fan, Y., Li, H., & Miguez-Macho, G. (2013). Global Patterns of Groundwater Table Depth.  
560 *Science*, 339(6122), 940–943. <https://doi.org/10.1126/science.1229881>
- 561 Frau, D., Moran, B. J., Arengo, F., Marconi, P., Battauz, Y., Mora, C., ... Boutt, D. F. (2021).  
562 Hydroclimatological Patterns and Limnological Characteristics of Unique Wetland  
563 Systems on the Argentine High Andean Plateau. *Hydrology*, 8(4), 164.  
564 <https://doi.org/10.3390/hydrology8040164>
- 565 Gamboa, C., Godfrey, L., Herrera, C., Custodio, E., & Soler, A. (2019). The origin of solutes in  
566 groundwater in a hyper-arid environment: A chemical and multi-isotope approach in the  
567 Atacama Desert, Chile. *Science of The Total Environment*, 690, 329–351.  
568 <https://doi.org/10.1016/j.scitotenv.2019.06.356>
- 569 Gajardo, G., & Redón, S. (2019). Andean hypersaline lakes in the Atacama Desert, northern  
570 Chile: Between lithium exploitation and unique biodiversity conservation. *Conservation*  
571 *Science and Practice*, 1(9), 1–8. <https://doi.org/10.1111/csp2.94>
- 572 Gayo, E. M., C. Latorre, T. E. Jordan, P. L. Nester, S. A. Estay, K. F. Ojeda, and C. M. Santoro  
573 (2012), Late Quaternary hydrological and ecological changes in the hyperarid core of the

574 northern Atacama Desert (~21°S), *Earth-Science Rev.*, 113(3-4), 120–140,  
575 doi:10.1016/j.earscirev.2012.04.003.

576 Ge, J., Chen, J., Ge, L., Wang, T., Wang, C., & Chen, Y. (2016). Isotopic and hydrochemical  
577 evidence of groundwater recharge in the Hopq Desert, NW China. *Journal of*  
578 *Radioanalytical and Nuclear Chemistry*, 310(2), 761–775.  
579 <https://doi.org/10.1007/s10967-016-4856-8>

580 Gleeson, T., L. Marklund, L. Smith, and A. H. Manning (2011), Classifying the water table at  
581 regional to continental scales, *Geophys. Res. Lett.*, 38(5), 1–6,  
582 doi:10.1029/2010GL046427

583 Gleeson, T., Wada, Y., Bierkens, M. F. P., & van Beek, L. P. H. (2012). Water balance of global  
584 aquifers revealed by groundwater footprint. *Nature*, 488(7410), 197–200.  
585 <https://doi.org/10.1038/nature11295>

586 Gleeson, T. (2020). Global Groundwater Sustainability. *Groundwater*, 58(4), 484–485.  
587 <https://doi.org/10.1111/gwat.12991>

588 Godfrey, L. V., Chan, L.-H., Alonso, R. N., Lowenstein, T. K., McDonough, W. F., Houston, J.,  
589 ... Jordan, T. E. (2013). The role of climate in the accumulation of lithium-rich brine in  
590 the Central Andes. *Applied Geochemistry*, 38, 92–102.  
591 <https://doi.org/10.1016/j.apgeochem.2013.09.002>

592 Grosjean, Martin; Geyh, Mebus A.; Messerli, Bruno; Schotterer, U. (1995). Late-glacial and  
593 early Holocene lake sediments, groundwater formation and climate in the Atacama  
594 Altiplano 22-24°S. *Journal of Paleolimnology*, 14, 241–252.

595 Gutiérrez, J. S., Navedo, J. G., & Soriano-Redondo, A. (2018). Chilean Atacama site imperilled  
596 by lithium mining. *Nature*, 557(7706), 492–492. [https://doi.org/10.1038/d41586-018-](https://doi.org/10.1038/d41586-018-05233-7)  
597 [05233-7](https://doi.org/10.1038/d41586-018-05233-7)

598 Hartley, A. J., and G. Chong (2002), Late Pliocene age for the Atacama Desert: Implications for  
599 the desertification of western South America, *Geology*, 30(1), 43–46, doi:10.1130/0091-  
600 7613(2002)030<0043:LPAFTA>2.0.CO;2.

601 Haitjema, H. M., and S. Mitchell-Bruker (2005), Are Water Tables a Subdued Replica of the  
602 Topography?, *Ground Water*, 43(6), 781–786, doi:10.1111/j.1745-6584.2005.00090.x.

603 Herrera, C., Custodio, E., Chong, G., Lambán, L. J., Riquelme, R., Wilke, H., ... Licteuvout, E.  
604 (2016). Groundwater flow in a closed basin with a saline shallow lake in a volcanic area:  
605 Laguna Tuyajto, northern Chilean Altiplano of the Andes. *Science of The Total*  
606 *Environment*, 541, 303–318. <https://doi.org/10.1016/j.scitotenv.2015.09.060>

607 Houston, J. (2002). Groundwater recharge through an alluvial fan in the Atacama Desert,  
608 northern Chile: mechanisms, magnitudes and causes. *Hydrological Processes*, 16(15),  
609 3019–3035. <https://doi.org/10.1002/hyp.1086>

610 Houston, J. (2007). Recharge to groundwater in the Turi Basin, northern Chile: An evaluation  
611 based on tritium and chloride mass balance techniques. *Journal of Hydrology*, 334(3–4),  
612 534–544. <https://doi.org/10.1016/j.jhydrol.2006.10.030>

- 613 Houston, J. (2009). A recharge model for high altitude, arid, Andean aquifers. *Hydrological*  
614 *Processes*, 23(16), 2383–2393. <https://doi.org/10.1002/hyp.7350>
- 615 Immerzeel, W. W., Lutz, A. F., Andrade, M., Bahl, A., Biemans, H., Bolch, T., ... Baillie, J. E.  
616 M. (2020). Importance and vulnerability of the world's water towers. *Nature*, 577(7790),  
617 364–369. <https://doi.org/10.1038/s41586-019-1822-y>
- 618 IPCC, 2022: Climate Change 2022: Impacts, Adaptation, and Vulnerability. Contribution of  
619 Working Group II to the Sixth Assessment Report of the Intergovernmental Panel on  
620 Climate Change [H.-O. Pörtner, D.C. Roberts, M. Tignor, E.S. Poloczanska, K.  
621 Mintenbeck, A. Alegría, M. Craig, S. Langsdorf, S. Löschke, V. Möller, A. Okem, B.  
622 Rama (eds.)]. Cambridge University Press. Cambridge University Press, Cambridge, UK  
623 and New York, NY, USA, 3056 pp., doi:10.1017/9781009325844.
- 624 Jasechko, S. (2016). Partitioning young and old groundwater with geochemical tracers. *Chemical*  
625 *Geology*, 427, 35–42. <https://doi.org/10.1016/j.chemgeo.2016.02.012>
- 626 Jordan, T., Lameli, C. H., Kirk-Lawlor, N., & Godfrey, L. (2015). Architecture of the aquifers of  
627 the Calama Basin, Loa catchment basin, northern Chile. *Geosphere*, 11(5), 1438–1474.  
628 <https://doi.org/10.1130/GES01176.1>
- 629 Kendall, C. & Caldwell, E.A. (1998) Fundamentals of isotope geochemistry. In: *Isotope Tracers*  
630 *in Catchment Hydrology* (Eds C. Kendall & J.J. McDonnell), pp. 51-86. Elsevier,  
631 Amsterdam.
- 632 Kendall, C., McDonnell, J.J. (1998). *Isotope Tracers in Catchment Hydrology*. 839 pp. Elsevier,  
633 New York
- 634 Kroepelin, S., Verschuren, D., Lezine, A.-M., Eggermont, H., Cocquyt, C., Francus, P., ...  
635 Engstrom, D. R. (2008). Climate-Driven Ecosystem Succession in the Sahara: The Past  
636 6000 Years. *Science*, 320(5877), 765–768. <https://doi.org/10.1126/science.1154913>
- 637 Liu, Y., Wagener, T., Beck, H. E., & Hartmann, A. (2020). What is the hydrologically effective  
638 area of a catchment? *Environmental Research Letters*, 15(10), 104024.  
639 <https://doi.org/10.1088/1748-9326/aba7e5>
- 640 Lucas, L., & Unterweger, M. (2000). Comprehensive review and critical evaluation of the half-  
641 life of tritium. *Journal of Research of the National Institute of Standards and Technology*,  
642 105(4), 541–549. <https://doi.org/10.6028/jres.105.043>
- 643 Masbruch, M. D., Rumsey, C. A., Gangopadhyay, S., Susong, D. D., & Pruitt, T. (2016).  
644 Analyses of infrequent (quasi-decadal) large groundwater recharge events in the northern  
645 Great Basin: Their importance for groundwater availability, use, and management. *Water*  
646 *Resources Research*, 52(10), 7819–7836. <https://doi.org/10.1002/2016WR019060>
- 647 Marconi, P., Arengo, F., & Clark, A. (2022). The arid Andean plateau waterscapes and the  
648 lithium triangle: flamingos as flagships for conservation of high-altitude wetlands under  
649 pressure from mining development. *Wetlands Ecology and Management*, (0123456789).  
650 <https://doi.org/10.1007/s11273-022-09872-6>
- 651 McKnight, S. V., Boutt, D. F., & Munk, L. A. (2021). Impact of Hydrostratigraphic Continuity  
652 on Brine-to-Freshwater Interface Dynamics: Implications From a Two-Dimensional

- 653 Parametric Study in an Arid and Endorheic Basin. *Water Resources Research*, 57(4).  
654 <https://doi.org/10.1029/2020WR028302>
- 655 McKnight, S. V., Boutt, D. F., Munk, L. A., & Moran, B. (2023). Distinct Hydrologic Pathways  
656 Regulate Perennial Surface Water Dynamics in a Hyperarid Basin. *Water Resources*  
657 *Research*, 59(4). <https://doi.org/10.1029/2022WR034046>
- 658 Mehran, A., Mazdiyasi, O. & AghaKouchak, A. A hybrid framework for assessing  
659 socioeconomic drought: Linking climate variability, local resilience, and demand. *J.*  
660 *Geophys. Res. Atmos.* 120, 7520–7533 (2015)
- 661 Mehran, A., AghaKouchak, A., Nakhjiri, N. et al. Compounding Impacts of Human-Induced  
662 Water Stress and Climate Change on Water Availability. *Sci Rep* 7, 6282 (2017).  
663 <https://doi.org/10.1038/s41598-017-06765-0>
- 664 Moran, B. J., Boutt, D. F., & Munk, L. A. (2019). Stable and Radioisotope Systematics Reveal  
665 Fossil Water as Fundamental Characteristic of Arid Orogenic-Scale Groundwater  
666 Systems. *Water Resources Research*, 55(12), 11295–11315.  
667 <https://doi.org/10.1029/2019WR026386>
- 668 Moran, Brendan J.; Boutt, David F.; McKnight, Sarah V.; Jenckes, Jordan; Munk, Lee Ann;  
669 Corkran, Daniel; and Kirshen, Alexander, "Data for "Relic Groundwater and Mega  
670 Drought Confound Interpretations of Water Sustainability and Lithium Extraction in Arid  
671 Lands"" (2021). Data and Datasets. 145. <https://scholarworks.umass.edu/data/145>
- 672 Munk, L.A., Hynek, S.A., Bradley, D.C., Boutt, D.F., Labay, K., Jochens, H., (2016). Lithium  
673 Brines: A Global Perspective, in Verplanck, P.L. and Hitzman, M.W., eds., *Rare Earth*  
674 *and Critical Elements in Ore Deposits. Reviews in Economic Geology* (18), 339–365.
- 675 Munk, L. A., Boutt, D. F., Hynek, S. A., & Moran, B. J. (2018). Hydrogeochemical fluxes and  
676 processes contributing to the formation of lithium-enriched brines in a hyper-arid  
677 continental basin. *Chemical Geology*, 493, 37–57.  
678 <https://doi.org/10.1016/j.chemgeo.2018.05.013>
- 679 Munk, L. A., Boutt, D. F., Moran, B. J., McKnight, S. V., & Jenckes, J. (2021). Hydrogeologic  
680 and geochemical distinctions in freshwater-brine systems of an Andean salar.  
681 *Geochemistry, Geophysics, Geosystems*, 22, e2020GC009345.  
682 <https://doi.org/10.1029/2020GC009345>
- 683 Panichi C. and Gonfiantini R.. Environmental isotopes in geothermal studies. *Geothermics*  
684 1977;6(3-4):143-161. [https://doi.org/10.1016/0375-6505\(77\)90024-4](https://doi.org/10.1016/0375-6505(77)90024-4)
- 685 Pfeiffer, M., Latorre, C., Santoro, C. M., Gayo, E. M., Rojas, R., Carrevedo, M. L., ...  
686 Amundson, R. (2018). Chronology, stratigraphy and hydrological modelling of extensive  
687 wetlands and paleolakes in the hyperarid core of the Atacama Desert during the late  
688 quaternary. *Quaternary Science Reviews*, 197, 224–245.  
689 <https://doi.org/10.1016/j.quascirev.2018.08.001>
- 690 Placzek, C. J., J. Quade, and P. J. Patchett (2013), A 130ka reconstruction of rainfall on the  
691 Bolivian Altiplano, *Earth Planet. Sci. Lett.*, 363, 97–108, doi:10.1016/j.epsl.2012.12.017.

- 692 Rech, J. A., Currie, B. S., Jordan, T. E., Riquelme, R., Lehmann, S. B., Kirk-Lawlor, N. E., ...  
693 Gooley, J. T. (2019). Massive middle Miocene gypsic paleosols in the Atacama Desert  
694 and the formation of the Central Andean rain-shadow. *Earth and Planetary Science*  
695 *Letters*, 506, 184–194. <https://doi.org/10.1016/j.epsl.2018.10.040>
- 696 Rissmann, C., Leybourne, M., Benn, C., & Christenson, B. (2015). The origin of solutes within  
697 the groundwaters of a high Andean aquifer. *Chemical Geology*, 396, 164–181.  
698 <https://doi.org/10.1016/j.chemgeo.2014.11.029>
- 699 Rooyen, J. D., Watson, A. P., Palcsu, L., & Miller, J. A. (2021). Constraining the Spatial  
700 Distribution of Tritium in Groundwater Across South Africa. *Water Resources Research*,  
701 57(8). <https://doi.org/10.1029/2020WR028985>
- 702 Scanlon, B. R., Keese, K. E., Flint, A. L., Flint, L. E., Gaye, C. B., Edmunds, W. M., &  
703 Simmers, I. (2006). Global synthesis of groundwater recharge in semiarid and arid  
704 regions. *Hydrological Processes*, 20(15), 3335–3370. <https://doi.org/10.1002/hyp.6335>
- 705 Scheihing, K. W., Moya, C. E., Struck, U., Lictevout, E., & Tröger, U. (2018). Reassessing  
706 hydrological processes that control stable Isotope Tracers in groundwater of the Atacama  
707 Desert (Northern Chile). *Hydrology*, 5(1). <https://doi.org/10.3390/hydrology5010003>.
- 708 Somers, L. D., & McKenzie, J. M. (2020). A review of groundwater in high mountain  
709 environments. *WIREs Water*, 7(6). <https://doi.org/10.1002/wat2.1475>
- 710 Sonter, L. J., Dade, M. C., Watson, J. E. M., & Valenta, R. K. (2020). Renewable energy  
711 production will exacerbate mining threats to biodiversity. *Nature Communications*, 11(1),  
712 4174. <https://doi.org/10.1038/s41467-020-17928-5>
- 713 Stewart, M. K., Morgenstern, U., Gusyev, M. A., & Maloszewski, P. (2017). Aggregation effects  
714 on tritium-based mean transit times and young water fractions in spatially heterogeneous  
715 catchments and groundwater systems, and implications for past and future applications of  
716 tritium. *Hydrology and Earth System Sciences Discussions*, (October), 1–26.  
717 <https://doi.org/10.5194/hess-2016-532>
- 718 Viguiier, B., Jourde, H., Leonardi, V., Lictevout, E., & Daniele, L. (2020). Water table variations  
719 in Atacama desert alluvial fans: Discussion of “evidence of short-term groundwater  
720 recharge signal propagation from the Andes to the central Atacama desert: A singular  
721 spectrum analysis approach.” *Hydrological Sciences Journal*, 65(9), 1606–1613.  
722 <https://doi.org/10.1080/02626667.2020.1764001>
- 723 Walvoord, M. A., Plummer, M. A., Phillips, F. M., & Wolfsberg, A. V. (2002). Deep arid system  
724 hydrodynamics 1. Equilibrium states and response times in thick desert vadose zones.  
725 *Water Resources Research*, 38(12), 44-1-44–15. <https://doi.org/10.1029/2001WR000824>
- 726 Wang, J., Song, C., Reager, J. T., Yao, F., Famiglietti, J. S., Sheng, Y., ... Wada, Y. (2018).  
727 Recent global decline in endorheic basin water storages. *Nature Geoscience*, 11(12), 926–  
728 932. <https://doi.org/10.1038/s41561-018-0265-7>
- 729 Wheeler, H., Sorooshian, S., & Sharma, K. (Eds.). (2007). *Hydrological Modelling in Arid and*  
730 *Semi-Arid Areas (International Hydrology Series)*. Cambridge: Cambridge University  
731 Press. doi:10.1017/CBO9780511535734

732 Wood, C., Cook, P. G., & Harrington, G. A. (2015). Vertical carbon-14 profiles for resolving  
733 spatial variability in recharge in arid environments. *Journal of Hydrology*, 520, 134–142.  
734 <https://doi.org/10.1016/j.jhydrol.2014.11.044>

735 Zipper, S. C., Jaramillo, F., Wang-Erlandsson, L., Cornell, S. E., Gleeson, T., Porkka, M., ...  
736 Gordon, L. (2020). Integrating the Water Planetary Boundary With Water Management  
737 From Local to Global Scales. *Earth's Future*, 8(2).  
738 <https://doi.org/10.1029/2019EF001377>

### 739 **Acknowledgments**

740 The authors would like to thank Felicity Arengo, Patricia Marconi, and Diego Frau for inviting  
741 us to join multiple sampling campaigns that were pivotal to collecting the data that initiated this  
742 study on the Puna. We also want to thank Ricki Sheldon, the Consejo de Pueblos Atacameños,  
743 Asociación de Agricultores Zapar, Asociación de Agricultores Soncor, Comunidad de Toconao,  
744 Comunidad de Catarpe, Comunidad de Coyo, Familia Bautista de Tambillo, and CONAF for  
745 graciously volunteering to access and conduct sampling that was pivotal to this study.

### 746 **Author Contributions**

747 Conceptualization, B.M.; Methodology, B.M., D.B.; Formal Analysis, B.M.; Investigation, B.M.,  
748 D.B., L.M.; Resources, D.B., L.M., J.F.; Writing – Original Draft Preparation, B.M.; Writing –  
749 Review & Editing, B.M., D.B., L.M., J.F.; Funding Acquisition, B.M., D.B., L.M., J.F.

### 750 751 **Competing Interests**

752 The authors declare no competing interests.

### 753 **Supplementary Information**

754 Included in a separate document with this submission.